Electronic Supplementary Material (ESI) for Journal of Materials Chemistry A.


Electronic Supporting Information

# Electrocatalytic hydrogen evolution using graphitic carbon nitride coupled with nanoporous graphene co-doped by S and Se

S.S. Shinde, Abdul Sami, Jung-Ho Lee*

Department of Materials and Chemical Engineering,

Hanyang University, Ansan, Kyunggido, 426-791, Korea

E-mail: jungho@hanyang.ac.kr, Phone: +82-31-400-5278, Fax: +82-31-419-7203

## Results and discussion

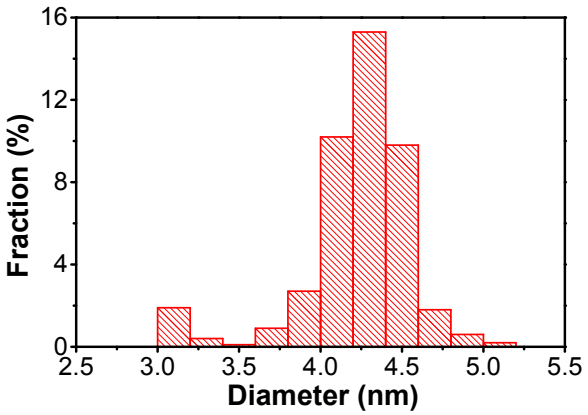


**Figure S1** Size distribution of graphene quantum dots detached from graphene matrix

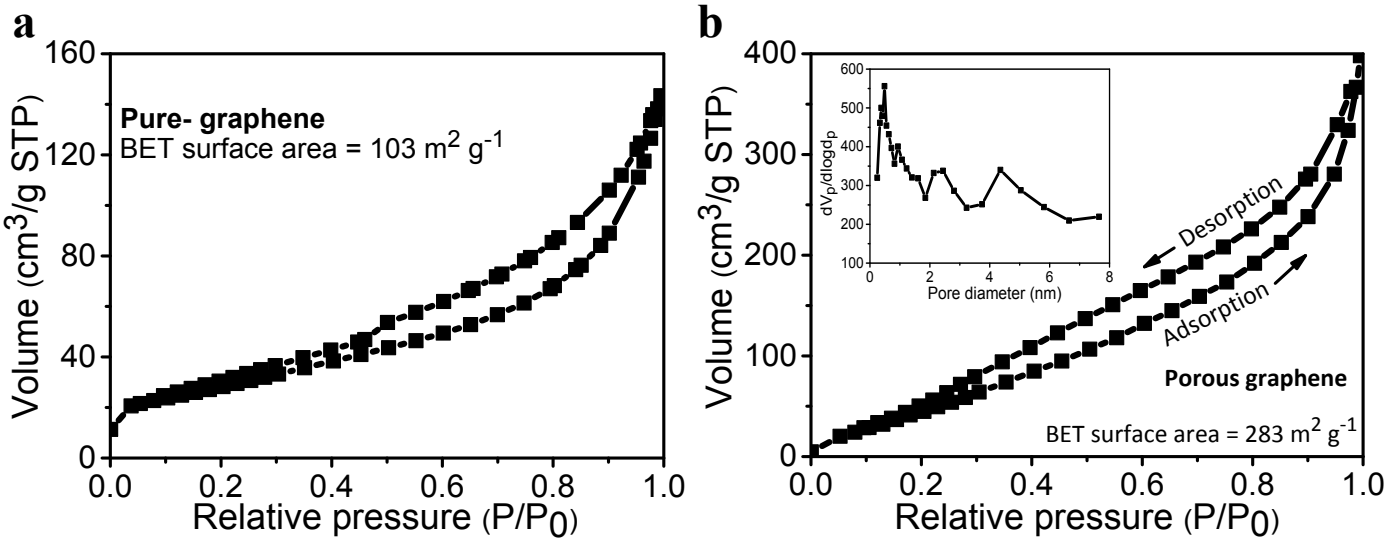


**Figure S2** Nitrogen adsorption isotherms and BET surface areas of (a) pure graphene and (b) nanoporous graphene; the inset shows a corresponding pore size distribution curve.

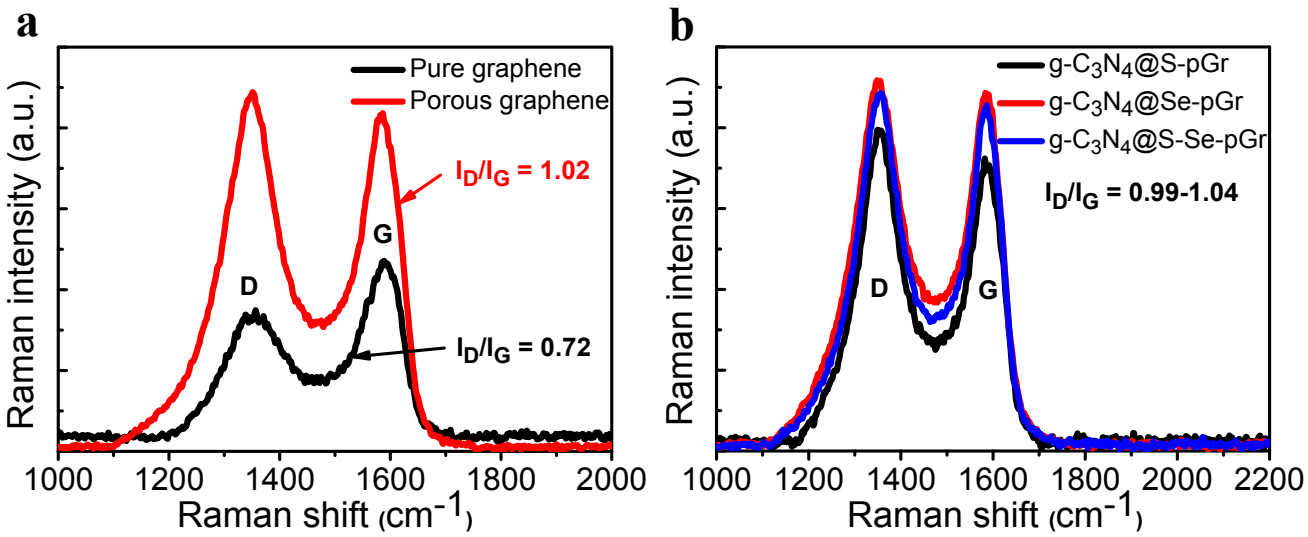


**Figure S3** Raman spectra of pure and porous graphene (a) and hybrid catalysts (b) and their $I_D/I_G$ ratios.

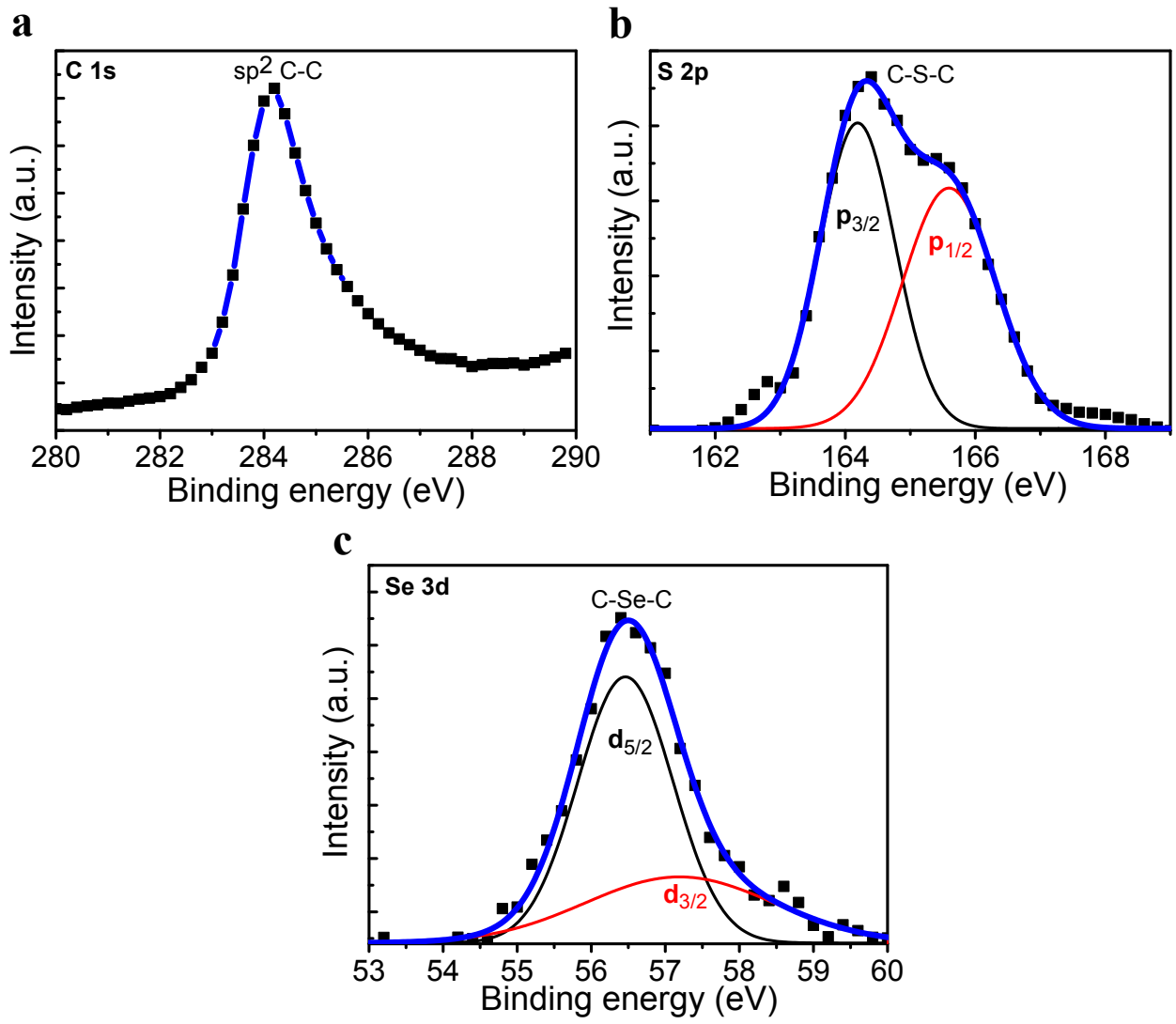


**Figure S4** High-resolution XPS spectra of (a) carbon in pristine graphene and (b) sulfur and (c) selenium in doped hybrid.

**Normalization process**

To normalize the activity in relation to the surface area and catalyst load (mass) for newly developed metal-free catalysts, we calculated the electrochemical active surface areas by measuring their electrochemical double-layer capacitances ($C_{dl}$) using a simple CV method. A potential range of 0.025-0.325 V vs. RHE was selected for the capacitance measurements because no electrochemical features corresponding to Faradic current were observed in this region. Then, the capacitive currents, i.e., $\Delta J_{|Ja-Jc|}$ @0.2 V, were plotted as a function of the CV scan rate, as shown in Figs. S5 a,b; linear relationships were observed with slopes that were two times larger than the $C_{dl}$ value. Accordingly, the calculated $C_{dl}$ values of metal-free catalyst are shown in Table S3. Considering the catalyst load and electrochemical active surface area, the normalization of exchange current density is reported in Tables S3&4 in comparison with well-developed nanostructured $MoS_2$-based metallic catalysts.

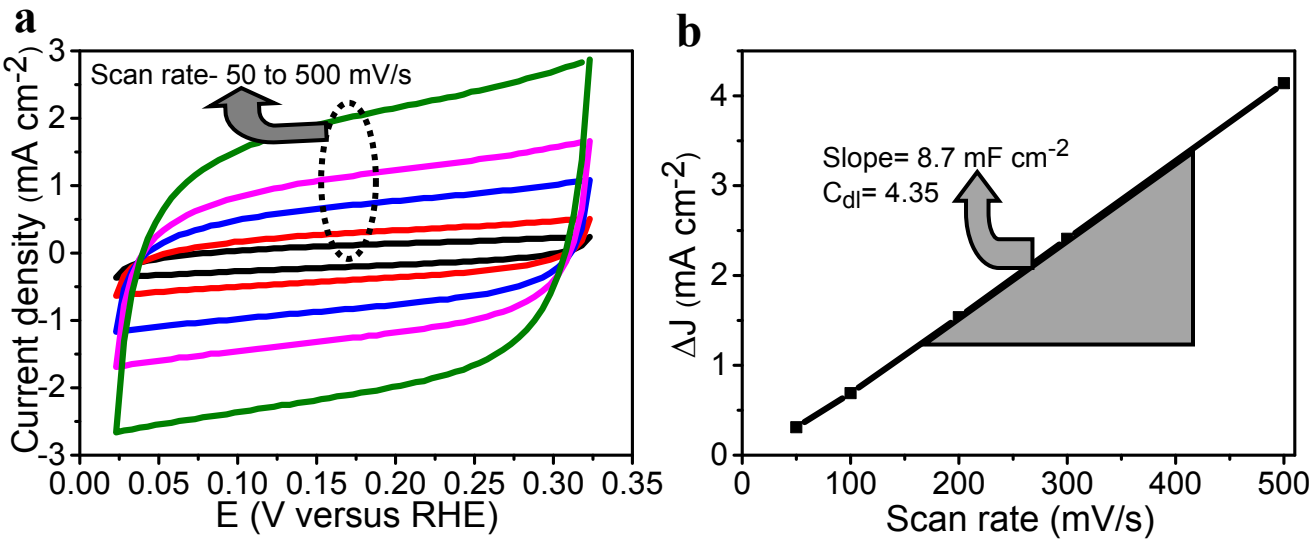


**Figure S5** (a) CV curves and (b) the corresponding difference in current density at 0.2 V plotted against scan rate of typical g-$C_3N_4$@S-Se-pGr catalyst; the calculated $C_{dl}$ values for different catalysts are shown in Table S3.

**Table S1** Electrochemical analysis of different catalysts (compared with reported literature) based on the polarization curves and Tafel plots (in 0.5 M $H_2SO_4$). The on-set potential in this study is defined as the overpotential at which the reduction current density is 0.5 mA/cm$^2$.

| Catalyst | On-set potential (V, versus RHE) | $\eta$ @ 10 mA cm$^{-2}$ (V, versus RHE) | Tafel value (mV/dec) | Reference |
|---|---|---|---|---|
| $C_3N_4$@NG | - | -0.240 | 51.1 | 1 |
| $C_3N_4$/NG | - | -0.380 | 67 | 1 |
| N-G | 0.331 | -0.490 | 116 | 2 |
| P-G | 0.374 | -0.553 | 133 | 2 |
| N,P-G | 0.289 | -0.420 | 91 | 2 |
| g-$C_3N_4$ nanoribbon-G | 0.080 | -0.207 | 54 | 3 |
| Graphene (500 $^o$C) | 0.50 | -0.661 | 237 | 4 |
| S-G (500 $^o$C) | 0.25 | -0.391 | 130 | 4 |
| N,S-G | 0.130 | -0.276 | 81 | 4 |
| Activated carbon nanotubes | 0.100 | - | 71.3 | 5 |
| Nitrogen-doped Activated Carbon | - | -0.625 | - | 6 |
| Monolayer $MoS_2$/NPG | 0.120 | -0.226 | 46 | 7 |
| $MoS_2$/RGO | - | -0.140 | 41 | 8 |
| S-pGr | 0.382 | -0.671 | 124 | This work |
| Se-pGr | 0.417 | -0.707 | 123 | This work |
| S-Se-pGr | 0.332 | -0.634 | 105 | This work |
| g-$C_3N_4$@S-pGr | 0.132 | -0.346 | 84 | This work |
| g-$C_3N_4$@Se-pGr | 0.162 | -0.398 | 93 | This work |
| g-$C_3N_4$@S-Se-pGr | 0.092 | -0.300 | 86 | This work |

**Table S2** Electrochemical analysis of different catalysts based on the polarization curves and Tafel plots (in 0.1 M KOH). The on-set potential in this study is defined as the overpotential at which the reduction current density is 0.5 mA/cm$^2$.

| **Catalyst** | **On-set potential (V, versus RHE)** | **$\eta$ @ 5 mA cm$^{-2}$ (V, versus RHE)** | **Tafel value (mV/dec)** | **$I_0$ (A cm$^{-2}$), ×10$^{-7}$** |
|---|---|---|---|---|
| S-pGr | 0.340 | -1.24 | 212 | 2.25 |
| Se-pGr | 0.180 | -1.31 | 203 | 1.44 |
| S-Se-pGr | 0.665 | -1.19 | 210 | 1.82 |
| g-$C_3N_4$@S-pGr | 0.420 | -0.88 | 170 | 4.83 |
| g-$C_3N_4$@Se-pGr | 0.380 | -0.97 | 174 | 2.87 |
| g-$C_3N_4$@S-Se-pGr | 0.320 | -0.86 | 169 | 5.58 |

**Table S3** Comparison of catalyst loading, exchange current density, and electrochemical active surface area for the currently reported HER catalysts.

| **Catalyst** | **Catalyst loading ($\mu g/cm^2$)** | **$I_0$ ($A\ cm^{-2}$), $\times 10^{-6}$** | **$C_{dl}$ ($mF\ cm^{-2}$)** | **Reference** |
|---|---|---|---|---|
| $C_3N_4$@NG hybrid | 100 | 0.35 | 5 | 1 |
| N,P-G | 200 | 0.24 | 10.6 | 2 |
| g-$C_3N_4$ nanoribbon-G | 143 | 23700 | 13 | 3 |
| N,S-G | - | 8.4 | - | 4 |
| $MoS_2$/RGO | 285 | 5.10 | 2.40 | 9 |
| $MoO_3$-$MoS_2$ | 60 | 8.20 | 2.20 | 9 |
| Amorphous $MoS_x$ | 9 | 0.15 | 1.10 | 9 |
| $MoS_2$/graphene | 210 | 3.00 | 10.4 | 10 |
| Amorphous $MoS_2$ | ~31 | 0.89 | 2.30 | 11 |
| $MoS_2$ nanosheet | 285 | 12.6 | 33.7 | 12 |
| S-pGr | 20 | 0.90 | 13.3 | This work |
| Se-pGr | 20 | 2.34 | 14.1 | This work |
| S-Se-pGr | 20 | 2.29 | 3.89 | This work |
| g-$C_3N_4$@S-pGr | 20 | 5.59 | 5.75 | This work |
| g-$C_3N_4$@Se-pGr | 20 | 2.61 | 6.73 | This work |
| g-$C_3N_4$@S-Se-pGr | 20 | 6.27 | 4.35 | This work |

**Table S4** Exchange current densities normalized in relation to the catalyst load (mass), active surface area and mass, and area for various catalysts.

| Catalyst | $I_0$ (A $cm^{-2}$) normalized by mass, $\times10^{-6}$ | $I_0$ (A $cm^{-2}$) normalized by area, $\times10^{-6}$ | $I_0$ normalized by mass and area | Reference |
|---|---|---|---|---|
| $C_3N_4$@NG hybrid | 0.35 | 0.35 | 0.35E-6 | 1 |
| N,P-G | 0.12 | 0.12 | 0.24E-6 | 2 |
| g-$C_3N_4$ nanoribbon-G | 16753 | 16753 | 16.7E-3 | 3 |
| $MoS_2$/RGO | 1.79 | 2.40 | 8.42E-7 | 9 |
| $MoO_3$-$MoS_2$ | 13.7 | 3.54 | 5.89E-6 | 9 |
| Amorphous $MoS_x$ | 1.70 | 3.23 | 3.59E-7 | 9 |
| $MoS_2$/graphene | 1.43 | 1.44 | 3.00E-6 | 10 |
| Amorphous $MoS_2$ | 2.87 | 1.93 | 0.60E-6 | 11 |
| $MoS_2$ nanosheet | 4.42 | 1.90 | 5.30E-6 | 12 |
| S-pGr | 4.48 | 0.85 | 4.23E-6 | This work |
| Se-pGr | 11.7 | 2.34 | 1.17E-5 | This work |
| S-Se-pGr | 11.5 | 0.63 | 3.16E-6 | This work |
| g-$C_3N_4$@S-pGr | 28.0 | 2.28 | 1.14E-5 | This work |
| g-$C_3N_4$@Se-pGr | 13.1 | 1.25 | 6.24E-6 | This work |
| g-$C_3N_4$@S-Se-pGr | 31.4 | 1.94 | 9.68E-6 | This work |

Considering the influence of catalyst loading (minimum quantity compared to reported literature) and electrochemical active surface area of the hybrid catalyst, the activity of the prepared hybrids is “comparable” to those of the well-developed metallic (i.e., $MoS_2$, $MoO_3$, $MoS_x$) and metal-free (N, P, S doped, N/P, N/S dual doped graphene, $C_3N_4$@NG hybrid, activated carbon nanotubes) catalysts.

**References**


1 Y. Zheng, Y. Jiao, Y. Zhu, L. Li, Y. Han, Y. Chen, A. Du, M. Jaroniec, S. Zhang Qiao, *Nat. Commun.,* 2014, **5,** 3783.

2 Y. Zheng, Y. Jiao, L. Li, T. Xing, Y. Chen, M. Jaroniec, S. Zhang Qiao, *ACS Nano,* 2014, **8,** 5290

3 Y. Zhao, F. Zhao, X. Wang, C. Xu, Z. Zhang, G. Shi, L. Qu, *Angew. Chem. Int. Ed.,* 2014, **53,** 13934.

4 Y. Ito, W. Cong, T. Fujita, Z. Tang, M. Chen, *Angew. Chem. Int. Ed.,* 2015, **54,** 2131.

5 W. Cui, Q. Liu, N. Cheng, A. Asiricd, X. Sun, *Chem. Commun.,* 2014, **50,** 9340.

6 B. Zhang, Z. Wen, S.Ci, J. Chen, Z. He, *RSC Adv.,* 2014, **4,** 49161.

7 Y. Tan, P. Liu, L. Chen, W. Cong, Y. Ito, J. Han, X. Guo, Z. Tang, T. Fujita, A. Hirata, M. Chen, 2014, **26,** 8023.

8 X. Zheng, J. Xu, K. Yan, H. Wang, Z. Wang, S. Yang, Chem. Mater., 2014, **26,** 2344.

9 J. Kibsgaard, Z. Chen, B. N. Reinecke, T. F. Jaramillo, *Nat. Mater.*, 2012, **11,** 963.

10 L. Liao, J. Zhu, X. Bian, L. Zhu, M. Scanlon, H. Girault, B. Liu, *Adv. Funct. Mater.*, 2013, **23,** 5326

11 D. Merki, H. Vrubel, L. Rovelli, S. Fierroa, X. Hu, *Chem. Sci.*, 2012, **3,** 2515

12 J. Xie, J. Zhang, S. Li, F. Grote, X. Zhang, H. Zhang, R. Wang, Y. Lei, B. Pan, Y. Xie, *J. Am. Chem. Soc.*, 2013, **135,** 17881